Mitochondria serve as axonal shuttle for Cox7c mRNA through mechanism that involves its mitochondrial targeting signal

Bar Cohen[1,*], Adi Golani-Armon [1,2,*], Topaz Altman[3,*], Anca F. Savulescu[4], Musa M. Mhlanga[4,5], Eran Perlson[3,**] and Yoav S. Arava[1,**]

1- Faculty of Biology, Technion – Israel Institute of Technology, Israel
2- Faculty of Nanosciences and Nanoengineering, Technion – Israel Institute of Technology, Israel
3- Sackler Faculty of Medicine, Tel Aviv University, Israel
4- Division of Chemical, Systems & Synthetic Biology, Department of Integrative Biomedical Sciences, Faculty of Health Sciences, Institute of Infectious Disease & Molecular Medicine, University of Cape Town, Cape Town, South Africa
5- Gene Expression and Biophysics Unit, Instituto de Medicina Molecular, Faculdade de Medicina Universidade de Lisboa, Lisbon, Portugal.

* These authors contributed equally to this work

** Corresponding authors: eranpe@tauex.tau.ac.il, arava@technion.ac.il,

Key words: mRNA localization, mRNA transport, mitochondria, mRNA encoding mitochondrial proteins, axons, axonal transport

Abstract

Localized protein synthesis plays a key role in spatiotemporal regulation of the cellular proteome. Neurons, which extend axons over long distances, heavily depend on this process. However, the mechanisms by which axonal mRNAs are transported to protein target sites are not fully understood. Here, we describe a novel role for mitochondria in shuttling a nuclear encoded mRNA along axons. Fractionation analysis and smFISH revealed that the mRNA encoding Cox7c protein is preferentially associated with mitochondria from a neuronal cell line and from primary motor neuron axons. Live cell imaging of MS2-tagged Cox7c or Cryab control mRNA in primary motor neurons further confirmed the preferential colocalization of Cox7c mRNA with mitochondria. More importantly, Cox7c demonstrated substantial co-transport with mitochondria along axons. Intriguingly, the coding region, rather than the 3'UTR, was found to be the key domain for the co-transport. Furthermore, we show that puromycin treatment as well as hindering the synthesis of the mitochondrial targeting signal (MTS) reduced the co-localization. Overall, our results reveal a novel mRNA transport mode which exploits mitochondria as a shuttle and translation of the MTS as a recognition feature. Thus, mitochondria may play a role in spatial regulation of the axonal transcriptome and self-sustain their own proteome at distant neuronal sites.

Introduction

Neurons extend axons over long distances and through a variety of extracellular microenvironments, forming unique compartmentalized sites with specific functions. These neuronal extensions rely on proper mitochondrial activity for their growth, function, and survival. Indeed, mitochondrial dysfunction can lead to neurodegeneration and motoneuron diseases (1–3). In addition to addressing metabolic and energetic needs, mitochondria also serve as important signaling hubs, and are required for local protein synthesis events (4–8). However, it is largely unknown how mitochondria replenish their proteome or alter it in response to local needs. This question is particularly intriguing for distant mitochondria, since most of their proteins are derived from nucleus-transcribed mRNAs, yet protein and mitochondria transport times from the soma are prolonged (9–11). These mitochondria are probably replenished by local synthesis of proteins, since mRNAs encoding mitochondrial proteins were identified at distant axonal sites and local synthesis appears necessary for mitochondrial function (12–19). An accepted model for transport of these mRNA to neuronal extensions involves the formation of RNA granules that shuttle through an interaction with kinesin motors (20–22). Recently, an endosome-mediated mechanism for protein replenishment was suggested, in which mRNAs encoding mitochondrial proteins are transported to distant sites through their association with Rab7-containing endosomes. These mRNAs are then locally translated, and the protein is targeted to nearby mitochondria (23).

Previous data demonstrating that mRNA are associated with mitochondria (24–28), and that miRNAs are associated with mitochondria along the axons (8) led us to propose a mitochondria-centric mechanism that is independent of other organelles. Specifically, we hypothesized that axonal mitochondria are physically associated with mRNAs encoding mitochondrial proteins. Moreover, we reasoned that these may co-transport along the axon. Consistent with that, we found significant association of several mRNAs encoding mitochondrial proteins with mitochondria from a neuronal cell line and primary motor neurons. MS2-tagging and live imaging of Cox7c (Cytochrome c oxidase subunit 7C, a component of complex IV of the respiratory chain) mRNA revealed significant co-transport with mitochondria. Intriguingly, the coding region and in particular translation of the mitochondrial targeting signal (MTS),

appeared key to mRNA localization and co-transport. Thus, Cox7c represents a novel mode of mRNA transport within axons.

Results

To examine the possibility that mitochondria may serve as an mRNA transport vehicle, we first performed a biochemical analysis of mRNA's association with mitochondria. Briefly, mitochondria from N2a, a mouse neuroblastoma cell line, were fractionated by differential centrifugation to purify the mitochondria. The fraction purity was verified by western analysis for compartmental protein markers, revealing an enrichment of the mitochondrial protein Atp5A and the absence of the cytosolic marker GAPDH (Fig. 1A, B). Furthermore, RT-qPCR for mRNAs transcribed inside the mitochondria: ND5 (encoding NADH Dehydrogenase, Subunit 5) and Cox1 (encoding Cytochrome c oxidase I) also revealed an enrichment of these mRNAs in the mitochondrial fraction (Fig. 1C). Next, we analyzed mRNAs that encode mitochondrial proteins and are transcribed in the nuclear genome. To this end, we selected mRNAs encoding components of the oxidative phosphorylation pathway; studies in yeast revealed that such mRNAs are enriched near mitochondria (28). Importantly, the selected mRNAs were previously found to be enriched in rodents' axons [(Cox4i1 (Cytochrome c oxidase subunit 4 isoform 1), Atp5k (ATP synthase subunit e), Cox7c (Cytochrome c oxidase subunit 7C)] (15, 19, 29, 30). As shown in Fig. 1D, these mRNAs appeared to be enriched in the mitochondrial fraction. Interestingly, other mRNAs that were found before in axon but do not encode proteins that reside in mitochondria, such as Cryab protein (α Crystallin B chain), Rplp0 (Ribosomal protein of the large subunit), and β actin were detected at low levels in the mitochondrial fraction. Although the significance of the association of these "hitchhikers" remains to be determined, all of them appear at lower levels than mRNAs encoding *bona fide* mitochondrial protein.

To validate the biochemical association data by an alternative approach, we performed smFISH analysis to visualize Cox7c, representative of mRNAs encoding proteins that are inserted into the mitochondria, and Cryab, a control mRNA. Each of these was co-labeled with RNA transcribed by the mitochondrial genome (Rnr1) as a mitochondria marker; although smFISH staining of intra-mitochondrial RNA yields low signal compared to other mitochondria markers, we opted to mark mitochondria by

the same experimental approach. In any event, the smFISH data revealed a higher co-localization for Cox7c than for Cryab (Fig. 1E), consistent with the fractionation results.

Next, we investigated whether this association occurs in mitochondria from axons of mouse motor neurons. To that end, we developed a protocol for isolating mitochondria with their associated mRNAs from primary spinal cord axons. Cells were extracted from embryonic spinal cords and grown on a porous membrane ("Modified Boyden Chamber") that enabled us to separate the axons from the cell bodies. Soma and axonal protrusions were then scraped (Fig. 1F) (8, 19). RT-PCR analysis confirmed the absence of soma-marker mRNA (Pol β) from the axonal fractions; however, a known axonal mRNA (β actin) was clearly detected in axonal fractions (Fig. 1G). A fractionation protocol was devised to fractionate axons to mitochondria and axoplasm; western analysis confirmed the absence of a cytosolic marker from the mitochondrial fraction and vice versa (Fig. 1H) and RT-qPCR revealed a significant enrichment for mRNAs encoded by the mitochondrial genome in the mitochondrial fraction (Fig. 1I). Importantly, although variation between biological repeats is apparent due to complexity of the protocol, axonal mRNAs encoding mitochondrial proteins (predominantly Cox7c and Cox4i1) appear enriched in the mitochondrial fraction, whereas those encoding non-mitochondrial proteins (Cryab, Rplp0, and β actin) are at similar levels in the mitochondrial and axoplasm fractions (Fig. 1J). Thus, mRNAs encoding mitochondrial proteins are associated with mitochondria from primary neurons axons.

To further substantiate this notion, we utilized the MS2 system (31) to tag candidate mRNAs and follow their position and transport by confocal live imaging. The complete coding region (CDS) of Cox7c and Cox4i1 (as representatives of highly associated candidates) and of Cryab (as a low association, control marker) were cloned in-frame to CFP in an MS2-loop bearing expression vector (Fig. 2A). Furthermore, the 3'UTR of each gene was cloned downstream to the MS2-loops. This yielded transcripts (designated 'Full') that contain the entire transcript of each gene tagged with multiple MS2 loops. Each construct was transfected into N2a cells together with a plasmid expressing MS2-binding protein fused to YFP (MCP-YFP). Confocal microscopy was used to measure co-localization with MitoTracker-red stained mitochondria (Fig. 2A). Quantification of the mRNA signals that co-localized with mitochondrial signals revealed about 25% co-localization for the control, parental vector that expresses only

the MS2 loops (Fig. 2B). This level is most likely due to the abundance of mitochondria and MCP-YFP and represents the basal background of the system. Nevertheless, the MS2 constructs expressing Cox7c or Cox4i1 exhibited significantly higher co-localization values. Co-localization of Cryab mRNA was non-significantly different from the control MS2-only mRNA. Overall, these data support the preferred association of nuclear encoded mitochondrial mRNAs with mitochondria in a neuronal cell line.

mRNAs co-travel with mitochondria along axons

We next introduced the plasmids with MS2-tagged genes and MCP-GFP by viral infection into primary spinal cord neurons (Fig. 2C). Live imaging using spinning disk confocal microscopy provided high spatial and temporal resolution of mitochondria and tagged mRNA localization. We selected Cox7c for detailed analysis since it showed the highest enrichment among all tested mRNAs, yet its localization mechanisms are totally unknown (compared to Cox4i1 that was extensively studied (29, 32, 33)). Cryab was used as a non-mitochondrial control mRNA. Notably, all Cox7c mRNA signals appeared to co-localize with mitochondria, while less than 50% of Cryab signals was co-localized. Furthermore, all moving mRNA signals of Cox7c were in complete concordance to mitochondria movement while only a small fraction of Cryab was co-transported with mitochondria (Fig. 2D, E and Suppl. Movie 1,2). Thus, mRNA encoding mitochondria proteins not only associate with axonal mitochondria, but also shuttle with them along the axon.

The coding region contains key co-transport determinants

To identify which mRNA regions are important for co-transport of Cox7c with mitochondria, either the Cox7c coding region (CDS) alone or the 3'UTR alone were cloned into an MS2-loop bearing expression vector and expressed in N2a cells. Northern blot analysis confirmed that all transcripts (Full, CDS only or 3’UTR only) are of the expected length (Supplementary Fig. 1A, B). As these variants are expressed as CFP-fusions, expression and localization was tested by western analysis (Supplementary Fig. 2). We note that while mRNA levels of all variants appeared similar (Supplementary Fig. 1B, C), western analysis for CFP protein levels revealed significantly higher expression by the 3’UTR only construct, suggesting regulation at the protein level (Supplementary Fig. 2A, B). Nevertheless, fractionation analysis (normalized to the total amounts of protein) confirmed the expected location of the CFP

reporter, i.e., the mature (m) form of Full and CDS variant were mitochondrial, whereas CFP encoded by the 3'UTR plasmid was mostly cytosolic (Supplementary Fig. 2C).

To determine the localization of these mRNA variants, N2a cells were transfected with these constructs and with the MCP-YFP plasmid. Live imaging (Fig. 3) revealed that whereas the mRNA carrying the CDS region exhibited similar co-localization values to those of the entire Cox7c mRNA ('Full'), the mRNA carrying only the 3'UTR region had a much lower association (Fig. 3A, B). This reveals that the coding region is sufficient to induce mitochondrial localization.

As an alternative approach to imaging, we biochemically fractionated the transfected cells into cytosolic and mitochondrial fractions. Fractions were subjected to either northern analysis to directly detect the localization of the mRNA moiety (Supplementary Figure 1B, D) or to western analysis for MCP-YFP, as a proxy for the amounts of mRNA in each fraction (Supplementary Figure 3). Both approaches revealed that the mitochondrial amounts of the CDS-only and the Full transcripts are much higher than the 3'UTR only (or the MS2 only control). This fractionation data further supports the live imaging data for a role for the coding region in mRNA localization to mitochondria.

Importantly, we introduced the deletion variants into primary motor neurons (Fig. 3C-D, Supplementary movies 3 and 4). Also here, the CDS-only co-localization signals appeared very similar to those of the Full construct. Furthermore, focusing on the moving mRNAs along the axons revealed that all of them are moving together with mitochondria. However, this was not the case for the 3'UTR variant: most of its signal did not correlate with the movement of mitochondria. Overall, these data reveal that elements within the coding region are important for co-transport of Cox7c transcript with mitochondria.

Co-localization is dependent on translation of the Mitochondrial Targeting Signal (MTS)

The effects imposed by the CDS region suggest that translation of protein sequences contribute to co-localization. We therefore tested the possible role of a translational process by treating cells with the translation inhibitor puromycin, which leads to dissociation of ribosomes from mRNAs. While no effect was apparent in the

MS2-only control, a significant reduction in mitochondrial association was observed for the mRNA expressing the complete Cox7c transcript (Fig. 4A, B).

Most mitochondria proteins are targeted to the mitochondria through an N-terminal Mitochondria Targeting Signal (MTS)(34). Previous studies in yeast revealed the importance of MTS translation for directing the mRNA to mitochondria proximity (25, 35). To assess whether this mechanism underlies mRNA association with axonal mitochondria, we generated a Cox7c variant with a deletion of the 15 amino acids that are predicted to serve as an N-terminal MTS (36) ('no MTS'). Western-blot analysis verified that this protein is expressed properly but that it is not imported into mitochondria (Supplementary Fig. 2B). Importantly, confocal imaging of mRNA localization in N2a cells revealed a significant reduction in co-localization with mitochondria compared with the full, MTS-containing mRNA (Fig. 4C). Consistently, fractionation analysis of MCP-YFP, as a proxy for the mRNA localization, revealed much lower localization to the 'no MTS' compared to the Full construct (Supplementary Figure 3B, C). To exclude the possibility that the deleted 45 nts mRNA sequence underlies targeting, we generated a Cox7c variant with a non-sense point mutation at the fifth codon of Cox7c ('STOP'), which leads to a premature translation termination but without any other change in the Cox7c mRNA sequence. Furthermore, since this STOP mutation abolishes translation of the entire Cox7c protein, we generated a construct with an alternative start codon downstream to the MTS (Alt. Start), i.e. a missense mutation at the start codon (AUG to AAG) and a start codon at the 16th codon were introduced. This leads to translation of Cox7c yet without its MTS. As seen in Fig. 4D, these two variants, which are almost identical to the natural Cox7c mRNA, show a clear decrease in mRNA co-localization. Thus, translation of the MTS itself, rather than the mRNA sequence or other Cox7c protein domain, directs Cox7c mRNA to mitochondria proximity.

Finally, introducing the 'STOP' construct to primary motor neurons revealed similar findings, i.e. reduced colocalization of mRNA particles with mitochondria (Figure 4E-F, Supplementary movie 5). Moreover, axonal co-transport of this mRNA is also reduced compared to the full Cox7c construct. Thus, translation of the MTS may play a role in mitochondria localization and (consequently) co-transport in primary motor neurons.

Discussion

The data presented here reveal a novel mode of mRNA transport in neurons. We propose a model (Fig. 4G) in which nuclear-encoded mitochondrial mRNA is associated and transported with axonal mitochondria. We describe new determinants, namely translation and the emerging MTS, for proper association and hence co-transport. Translation of a signal peptide is the main mechanism for mRNA targeting to the ER (37), and we previously reported a similar localization mode for mRNAs encoding mitochondrial proteins with mitochondria of yeast cells (24, 25, 35). Yet, to the best of our knowledge, involvement of these determinants in long distance traffic was never shown. It should be noted that MTS association with the mitochondria outer membrane is transient, as this moiety is quickly inserted into mitochondria matrix and usually cleaved off the protein (34). Thus, we propose that the MTS serves primarily homing purposes, and once the mRNA is in proximity to mitochondria additional mRNA regions are employed for long term anchoring. Such localization regions are usually located in 3'UTRs and interact with RNA binding proteins on the mitochondria outer membrane (21, 22, 38)(39). Indeed, a cis element located within the 3' UTR of another Cox-family member (CoxIV) was shown to mediate its axonal localization (29). Also herein, the mRNA with only Cox7c 3'UTR was found to have some association with mitochondria, and disrupting the MTS did not fully abolish axonal co-transport of the Cox7c 'no MTS' construct (Fig. 4). Thus, multiple, not necessarily mutually exclusive, mRNA regions may ensure mRNA association with mitochondria for long periods of time.

Notably, Harbauer *et al.* had found that Pink1 mRNA is co-transported with mitochondria in neurons (40). Together with the data presented herein, this suggests a broad phenomenon, in which mitochondria are associated with many mRNAs encoding mitochondria proteins. Thereby axonal mitochondria may be self-sustained with respect to their protein content, which will allow immediate response to local needs as mitochondria meander along changing axonal microenvironments. Furthermore, mitochondria might serve as a shuttle vector for diverse types of mRNA to neuronal extremities, and by that spatiotemporally regulate cellular proteome. Indeed, we find several mitochondria-unrelated mRNAs to have some association with mitochondria ("hitchhikers"). A general role for mitochondria in mRNA shuttling is yet to be determined by more sensitive, genome-wide approaches. Another open question at this

stage is whether the interaction of mRNA with mitochondria occurs already at the cell body, and association is maintained throughout the lifetime of the mRNA. While we did not observe any mRNA dissociations through the time course of our analysis, better temporal and spatial tools are needed to follow mRNA traffic along the entire neuron.

Recently, a study in retinal ganglion cells of *Xenopus* revealed an endosome-mediated mode of transport for two mRNAs (*lamnb* and *vdac2*) with roles in mitochondrial function (23). In addition, a genome-wide analysis in the plant pathogen *U. maydis* suggested that many more mitochondrial mRNA are transported by endosomes (41). Thus, multiple pathways may work in parallel to ensure sufficient protein content for mitochondria at sites distant from the cell body. Notably, lysosomes were found to efficiently shuttle a non-mitochondrial mRNA (β actin) in axons (42). Thus, mRNA trafficking by moving organelles emerges as a general concept in the neuronal transport of diverse mRNA types.

Author contributions

B.C., A.G., T.A., E.P. and Y.A. designed the work, B.C, A.G. and T.A. performed the experiments and analyzed the data, A.F.S. performed the smFISH experiments and analyses, M.M.M., E.P., and Y.A provided funding, facilities and guidance, E.P and Y.A. wrote the manuscript with input from co-authors.

Acknowledgments

We thank Profs. Shai Berlin (Technion) and Yaron Shavtal (Bar Ilan University) for cells and plasmids, Prof. Ishi Talmon (Technion) for advice, and members of our labs for ideas and support. This work was funded by the ISF (grant 1096/13)(YA), Adelis Brain Research grant 2023478 (YA) and ISF (grant 735/19) to (EP).

Methods

Animals

HB9::GFP (stock no. 005029) mice colony was originally obtained from Jackson Laboratories. The colony was maintained by breeding with ICR mice (Jackson Laboratories). Mice were genotyped by DNA extraction and PCR using a utilized kit. For experimental purposes, only WT embryos of pregnant mice (GFP negative) were taken for motor neuron cultures.

Animal experiments were performed under the supervision and approval of the Tel-Aviv University Committee for Animal Ethics.

Cell growth, transfection and treatments

Mouse neuroblastoma cells, (N2a), a kind gift from Prof. Shai Berlin, Technion, were cultured in DMEM supplemented with 10% Fetal Bovine Serum (FBS), 2% penicillin/streptomycin, and 2 mM L-glutamine, at 37 °C in 5% CO2 atmosphere. Cells were split every 2-3 days by trypsinization. For transfection experiments, cells were grown to 60% confluency and transfected using jetPRIME reagent (Polyplus, 11415) according to manufacturer's instructions. Protein synthesis inhibition treatments were performed by incubating the cells with 200 μg/ml puromycin in growth medium for 45 min before imaging.

Primary motor neuron culture

Motor neurons were cultured from E12.5 ICR mouse embryos as previously described (8). Briefly, spinal cords were dissected, incubated with trypsin for 10 minutes, and triturated. The neuron containing soup was collected through a cushion of BSA, and the pellet was resuspended and centrifuged through a 10.4% Optiprep gradient for 20 min at 760 xg with the brake turned off. The cells were collected from the interphase, centrifuged through a cushion of BSA, counted and plated. Motor neurons were grown and maintained at 37°C 5% CO_2 incubator, in complete neurobasal medium containing 2% B27, 2% horse serum, 25 μM beta-mercaptoethanol, 1% Penicillin-Streptomycin, and 1% Glutamax supplemented with 1 ng/ml GDNF, 0.5 ng/ml CNTF, and 1 ng/ml BDNF.

Lentiviral production and infection

Lentiviral constructs were produced in HEK cells using a second-generation packaging system with Gag-Pol and VSVG helpers. HEK cells were grown on a 100-mm dish at high confluence, replaced to antibiotics free medium and transfected with 10 µg of MS2 vector, 10 µg of MCP-GFP and 20µg of helper plasmids. Plasmids were placed in a calcium phosphate transfection mix (25 mM HEPES, 5 mM KCl, 140 mM NaCl, and 0.75 mM Na_2PO_4 with 125 mM $CaCl_2$) in 1 mL volume per plate. Medium was replaced 8 hours after transfection, and supernatants were harvested 2 days afterwards. Lentiviral particles were concentrated 10-fold by using the PEG virus precipitation kit and kept at −80°C until use. Viral infection was performed using 10–20 µl of lentivirus per microfluidic chamber.

Mitochondria fractionation from N2a cells

24 hours post-transfection, N2a cells were detached and washed with ice-cold phosphate buffered serum (PBS), and pelleted by centrifugation (600g for 5 minutes at 4°C). Cell pellet was resuspended in HM (0.6 M mannitol, 50 mM Tris-HCl pH=7.4, 5 mM MgAc, 100 mM KCl, 1 mM DTT, 1 gr/L BSA, 200 µg/ml CHX, 1 mM PMSF, 1 µM Leupeptin, 1 µM Pepstatin, 0.3 µM Aprotinin and 0.04 U/µl RiboLock RNase Inhibitor (ThermoFisher)), and lysed by 15-20 strokes of a Dounce homogenizer. Lysate was centrifuged twice (1,000g for 10 minutes at 4°C) to pellet intact cells and nuclei, and supernatant (designated "Total") was further centrifuged at 15,000g for 15 minutes at 4°C to obtain a cytosolic fraction (supernatant) and a mitochondrial fraction (pellet).

Axonal harvesting and mitochondrial fractionation

Porous membranes (“Modified Boyden chamber”) with 1µm pores were placed in a 6 well culture plate. The membranes were coated with poly-DL-ornithine (1.5 µg/mL in PBS) overnight at 37°C then with Laminin (3 µg/mL in DDW) for at least 2 hours at 37°C prior to motor neuron plating. Primary motor neurons were then plated on the membranes (10^6 neurons per a membrane insert) and grown with complete neurobasal media. After 10 days in vitro (DIV), membranes were washed 3 times with warm PBS, followed by gentle scraping of the axonal (bottom) part of the membrane into a tube containing mitochondria Homogenization Buffer (HM) (0.6 M mannitol, 50 mM Tris-

HCL pH 7.4, 5 mM MgAc, 100 mM KCl, 1 gr/L BSA, 200 μg/ml cycloheximide (CHX), 1 mM DDT, 1X Protease inhibitor cocktail (Roche) and 0.04 U/μl RiboLock RNase Inhibitor (ThermoFisher)). Four membranes were collected for each experimental repeat. Axons collected in HM were sub-fractionated to cytosolic (C) and mitochondrial (M) fractions by two cycles of 12,000g centrifugation for 15 minutes at 4°C.

Western blot analysis

Samples from N2a cells and primary motor neurons were lysed and fractionated in mitochondria Homogenization Buffer (or immediately lysed after axonal harvest for somatic fraction), and were boiled in mixed in 1:4 (v/v) 5× Laemmli sample buffer for 5 min at 95°C. Next, samples were loaded on polyacrylamide gel and blotted on nitrocellulose membrane. The membrane was blocked with 5% BSA (N2a samples) or 5% milk (primary motor neuron samples) in TBS-Tween for 1 hour. Membranes of N2a cells samples were incubated for 1 hour at room temperature (RT) with primary antibodies for ATP5A (1:1000, Abcam Ab119688) and GAPDH (1:2000, Abcam Ab181602). The membranes were next incubated with secondary antibodies against mouse (1:20000, Sigma A5906) or rabbit (1:20000, Sigma A9169) for 45 minutes at RT and were exposed to ECL imager after 5 min incubation with EZ-ECL reagent (Biological Industries). Membranes of primary motor neuron samples were incubated overnight at 4°C with primary antibodies for ERK1/2 (1:10000, Sigma Aldrich) and ATPB (1:1000, Abcam). The membranes were next incubated with secondary anti-HRP antibody (1:10000, Jackson Laboratories) for 2 hours at RT and were exposed to ECL imager after 5 min incubation with ECL reagent (Thermo Fisher).

RT-qPCR

RNA was extracted from all samples (fractionated cells or axons) using Trizol reagent according to the manufacturer's protocol. RNA was reverse transcribed using Maxima First Strand cDNA Synthesis kit (Thermo scientific). To verify fraction purity, cDNA was subjected to PCR amplification with β-actin and Polymerase β primers (Table 2) followed by gel electrophoresis. Quantification of target genes was performed by real-time qPCR using SYBR green (Thermo Scientific). Targets were normalized to β-actin

and Rplp0 mRNA levels, and $\log_2$ fold-change between mitochondrial and cytosolic fractions was calculated (ΔΔCt). All real-time (RT) primers are listed in Table 2.

Table 2: List of primers used for real-time PCR

Primer name	Primer sequence
Atp5k Fw	CTACAGTTACCTAAAACCCCGG
Atp5k Rv	TGTCATCTTGAGCTTCCGC
β-actin Fw	ATGGATGACGATATCGCTG
β-actin Rv	GTTGGTAACAATGCCATGTTC
Cox1 Fw	TCCAACTCATCCCTTGACATC
Cox1 Rv	TCCTGCTATGATAGCAAACACT
Cox4i1 Fw	ACTATGCTTTCCCCACTTACG
Cox4i1 Rv	CTTCTCCTTCTCCTTCAGCG
Cox7c Fw	AGCATGTTGGGCCAGAGT
Cox7c Rv	ACTGAAAACGGCAAATTCTT
Cryab Fw	ACTTCCCTGAGCCCCTTCTA
Cryab Rv	TGCTTCACGTCCAGATTCAC
Nd5 Fw	AACCACACCTAGCATTCCTAC
Nd5 Rv	CAGGCGTTGGTGTTGCAGGTA
Rplp0 Fw	GGACCCGAGAAGACCTCCTT
Rplp0 Rv	GCACATCACTCAGAATTTCAATGG

smFISH

Design and manufacture of RNA FISH probes for use in the single molecule FISH method were performed according to the protocol by (43). Multiple 20-mer oligonucleotide probes conjugated to dyes, targeting the following mRNAs: Rnr1, Cryab and Cox7c were purchased (Biosearch Technologies). The Rnr1 probes were conjugated to TAMRA dye and the Cryab and Cox7c probes were conjugated to Quasar-670 dye. N2a cells were fixed in 3.7 % formaldehyde for 15 min at 37°C followed by washes in PBS and overnight permeabilization in 70% ethanol at 4°C. Cells were rehydrated in wash buffer (10% formaldehyde, 2X SSC) for 5 min. Hybridization was conducted overnight in a humidified chamber at 37°C in

Hybridization buffer (10 % dextran sulfate, 1 µg/µl E.coli tRNA, 2 mM Vanadyl ribonucleoside complex, 0.02% RNAse-free BSA, 10 % formamide, 2X SSC) combined with 50 ng of the desired RNA probe. Cells were then washed three times (each wash 30 min at room temperature) with FISH wash buffer (10% formaldehyde, 2X SSC). Cells were then incubated in equilibration buffer (0.4% glucose, 2X SSC) for 5 min and counter stained with 1 µg/ml DAPI (4',6-diamidino-2-phenylindole; Life Technologies). Coverslips were mounted in imaging buffer (3.7 µg/µl glucose oxidase and 1U catalase in equilibration buffer) and imaged on a StellarVision microscope using Synthetic Aperture Optics (SAO).

Plasmid construction

All mouse CDS and 3'UTR used were amplified from mouse cDNA using the primers indicated in Table 1. Fragments were cloned into phage-cmv-cfp-24xms2 vector (Addgene plasmid # 40651) created by Robert Singer lab. CDS fragments (from start codon to penultimate codon) were inserted in frame, upstream to CFP at the AgeI and NotI sites (under CMV promoter). 3'UTR fragments were inserted downstream to the MS2 stem loops cassette at the ClaI site. Constructs designated as 'Full' contain both the CDS and 3'UTR of the respective gene. 'CDS' or '3'UTR' designations indicate constructs with only these regions of the gene (cloned at the above restriction sites) and the CFP reporter. Proper construction was confirmed by sequencing and proper transcripts' length was validated by northern blot. We note that all constructs contained 12 MS loops instead of the expected 24, presumably due to recombination during cloning.

MCP-YFP plasmid was a gift from Prof. Yaron Shav-Tal (Bar Ilan University). MCP plasmid used for axonal live-imaging was phage-ubc-nls-ha-tdMCP-gfp (Addgene plasmid # 40649).

Table 1: List of primers used for plasmid cloning

Primer name	**Primer sequence**
Cox4i1 CDS Fw	ATAAGCGGCCGCATGTTGGCTTCCAGAGC
Cox4i1 CDS Rv	ATGGACCGGTCGCTTCTTCCACTCATTCTT
Cox4i1 3'UTR Fw	ACATATCGATGAGCCCGCTGCCTG
Cox4i1 3'UTR Rv	TCCGATCGATCACCACGTAAACTGGTC

Cox7c CDS Fw	ATATGCGGCCGCATGTTGGGCCAGAGTAT
Cox7c CDS Rv	CAGCACCGGTCGTTTTTTAAGTAGCTGGTGT
Cox7c 3'UTR Fw	CCCGATCGATGGATATTTAATTCATCCCT
Cox7c 3'UTR Rv	GCCGATCGATCAGAGACGAGGCATTG
Cox7c CDS no-MTS Fw	ATATGCGGCCGCCACCATGGTTAGCCACTATGAGGAG
Cox7c CDS stop-MTS Fw	ATATGCGGCCGCCACCATGGTTTTGGGCTAGAGTAT
Cryab CDS Fw	ATTTGCGGCCGCATGGACATCGCCATCC
Cryab CDS Rv	CAATACCGGTACCTTCTTAGGGGCTGCG
Cryab 3'UTR Fw	CCCGATCGATATCCCCTTTCCTCATTG
Cryab 3'UTR Rv	GCCGATCGATCAGAGACGAGGCATTG

Motor neuron axonal transport in microfluidic chambers

Polydimethylsiloxane (PDMS) home-made microfluidic chambers (MFC) were casted as previously described (44). To enable motor neuron plating and medium exchange, four 6 mm wells were punched in the end of each channel surrounding the microfluidic grooves. The microfluidic devices were then cleaned, first with adhesive tape to remove dirt and then sterilized in 70% ethanol for 10 min. The microfluidic devices were then dried, and UV irradiated for 10 min, followed by attachment to a 35 mm FluoroDish glass-bottom dish. For primary motor neuron plating, 150,000 neurons were concentrated and seeded in 4 µL medium to allow adhesion, and after 45 minutes 25 ng/mL BDNF enriched complete neurobasal medium was added. Lentiviral constructs were added to the proximal compartment two hours post-plating. From DIV 2, a neurotrophic and volume gradient was maintained between the distal and proximal compartment to encourage axonal crossing. Neurons were grown between 6-8 days to allow axonal crossing and lentiviral expression and were then stained with 100 nM Mitotracker Deep-Red FM for 30 minutes at 37°C followed by 3 washes with warm medium. For live axonal transport, movies of 100 frames were collected at 3 second intervals from the distal part of the MFC grooves. The movies were obtained using a Nikon Ti microscope equipped with a Yokogawa CSU X-1 spinning disc and an Andor iXon897 EMCCD camera controlled by Andor IQ3 software and 60x oil objective.

Axonal transport colocalization analysis was performed as previously described (3, 8). Briefly, transport movies were analyzed with kymograph generation, using Kymo ToolBox ImageJ plugin. Colocalization was determined where an mRNA particle kymograph track overlapped with a track in the corresponding mitochondria kymograph. Moving particles were defined after movement of more than 10µm in a specific direction during the movie 5-minute duration.

Live imaging and analysis of N2a cells

N2a cells were seeded in 24-well glass-bottom plates at a density of 50,000 cells/well and allowed to grow for 24 hours. Cells were then transfected with MCP-YFP plasmid and one of the MS2 plasmids (0.25µg of each). Twenty-four hours after transfection, mitochondria were stained with 100 nM MitoTracker® Red CMXRos (ThermoFisher) for 30 minutes at 37°C and washed with PBS before confocal live imaging. Images were captured using the LSM 710 inverted confocal microscope (Zeiss) with 63X NA 1.4 oil immersion objective lens. Z-stack images were acquired with 0.5µm z-step size and image pixel size of 0.1µm.

mRNA signal detection and mitochondria colocalization quantification were performed using Imaris. Mitochondria signal was masked and segmented using the built-in surface algorithm in Imaris. mRNA spots of 0.5 µm diameter were detected using the built-in spot detecting function. To take into account high signal variability between cells and to ensure correct signal detection, thresholds were chosen manually. Spot was considered colocalized if at least half of it overlapped with the mitochondria surface detected. Image processing for display proposes was done using FIJI. To filter background noise the MCP channel was subjected to the FTT bandpass filter and background subtraction. The mitochondrial signal channel was subjected to background subtraction.

Statistical analysis

Statistics analysis was performed using build in tools in Microsoft Excel or GraphPad Prism, with specific tests indicated in each Figure legend.

Figures

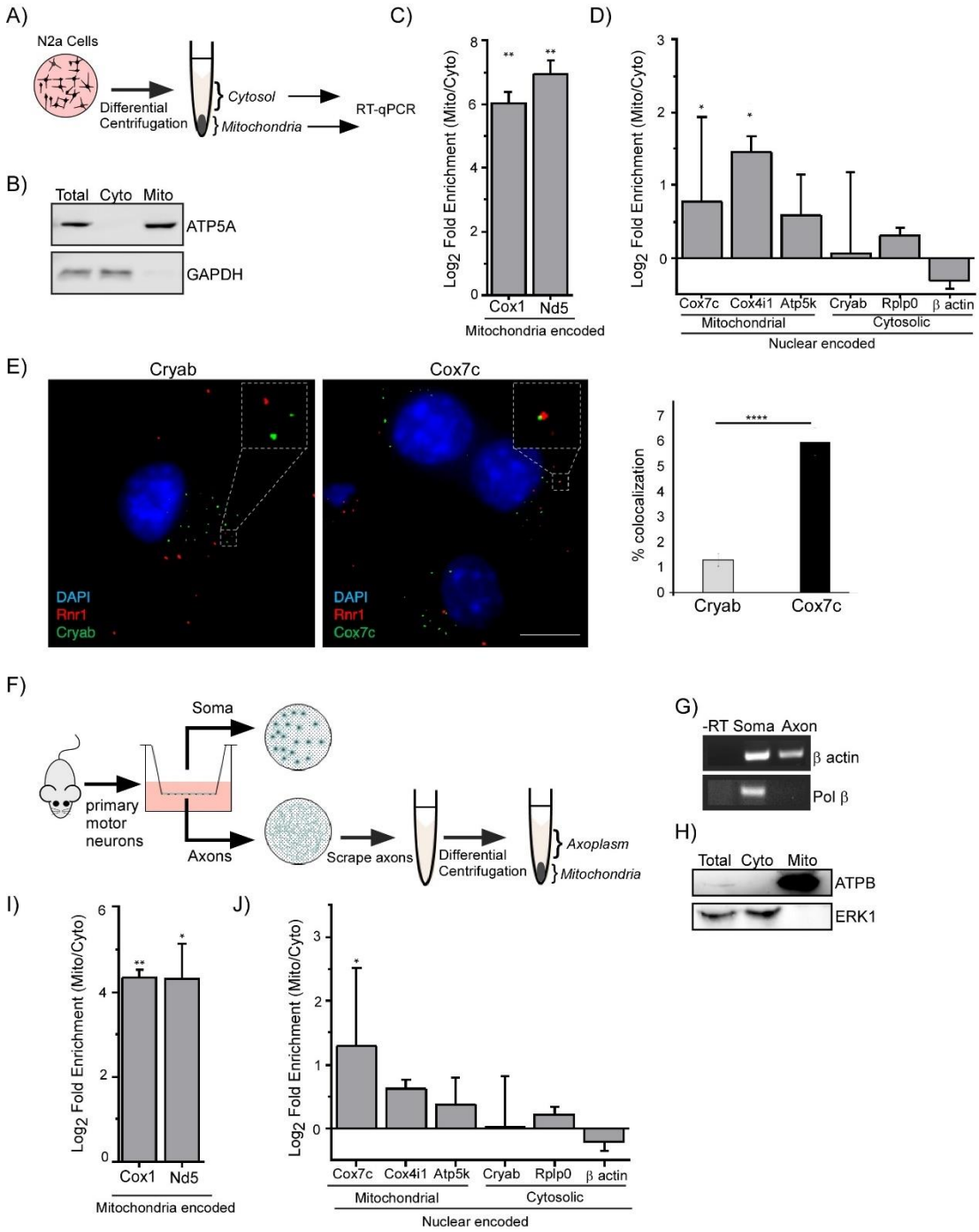

Figure 1: mRNAs encoding mitochondrial proteins are associated with mitochondria from N2a and motor neuron axons. A) Schematic workflow: N2a cells were collected and fractionated by differential centrifugation into cytosolic (Cyto) and mitochondrial (Mito) fractions followed by RNA purification and RT-qPCR. B) Western-blot analysis of the unfractionated total sample, cytosolic and mitochondrial fractions with a mitochondria marker (ATP5A) and cytosol marker (GAPDH), demonstrating fractionation purity. C) RT-qPCR analysis of mitochondrial and cytosolic fraction for mRNAs encoded inside the mitochondria. All values are

normalized to β-actin and Rplp0 transcript levels and presented as $\log_2$ fold enrichment of mitochondria and cytosolic Ct signals. Error bars are SEM. Two way-ANOVA, *p<0.05, **p<0.01. n = 4 independent biological repeats. D) RT-qPCR analysis of mitochondrial and cytosolic fraction for mRNAs encoded in the nucleus, separated to those that their proteins are destined to mitochondria or cytosol. Quantification as in panel C. Error bars are SEM. Two way-ANOVA, *p<0.05. n = 4 independent biological repeats. Scale bar = 5 μm. E) Representative images of smFISH done on N2a cells with the mRNA (green) of Cryab (left) or Cox7c (right). Probes targeting the 21S mitochondrial rRNA (Rnr1-red) were used to detect mitochondria signal. The histogram presents the percent of spots of each mRNA that colocalize with Rnr1 signals. Student's t-test, ****p<0.0001. For Cryab, 2027 spots from 82 cells were analyzed, and for Cox7c 1747 spots from 69 cells were analyzed, in three independent experiments. To minimize ambiguity, only spots with overlapping signals were considered as co-localized. F) Schematic workflow used for membrane-based compartmental isolation of primary motor neuron axons, and their fractionation into axoplasm (Cyto) and mitochondrial (Mito) fractions followed by RNA purification and RT-qPCR. G) RT-PCR analysis for soma-specific mRNA (Pol β) confirming separation purity. β actin represents mRNA present in both fractions. H) Western-blot analysis for fractionated axonal samples, with a mitochondrial marker (ATPB) and cytosolic marker (ERK1) demonstrating purity of mitochondria samples. I) RT-qPCR analysis was performed on axonal RNA samples from mitochondrial and axoplasm fractions for mRNAs encoded in the mitochondria. All values are normalized to β-actin and Rplp0 transcript levels. Error bars are SEM. Two-way ANOVA, *p<0.05. n = 3 independent biological repeats. J) RT-qPCR analysis of mitochondrial and cytosolic fractions for mRNAs encoded in the nucleus, separated to those that their proteins are destined to mitochondria or cytosol. Quantification as in panel I. Error bars are SEM. Two-way ANOVA, *p<0.05. n = 3 independent biological repeats.

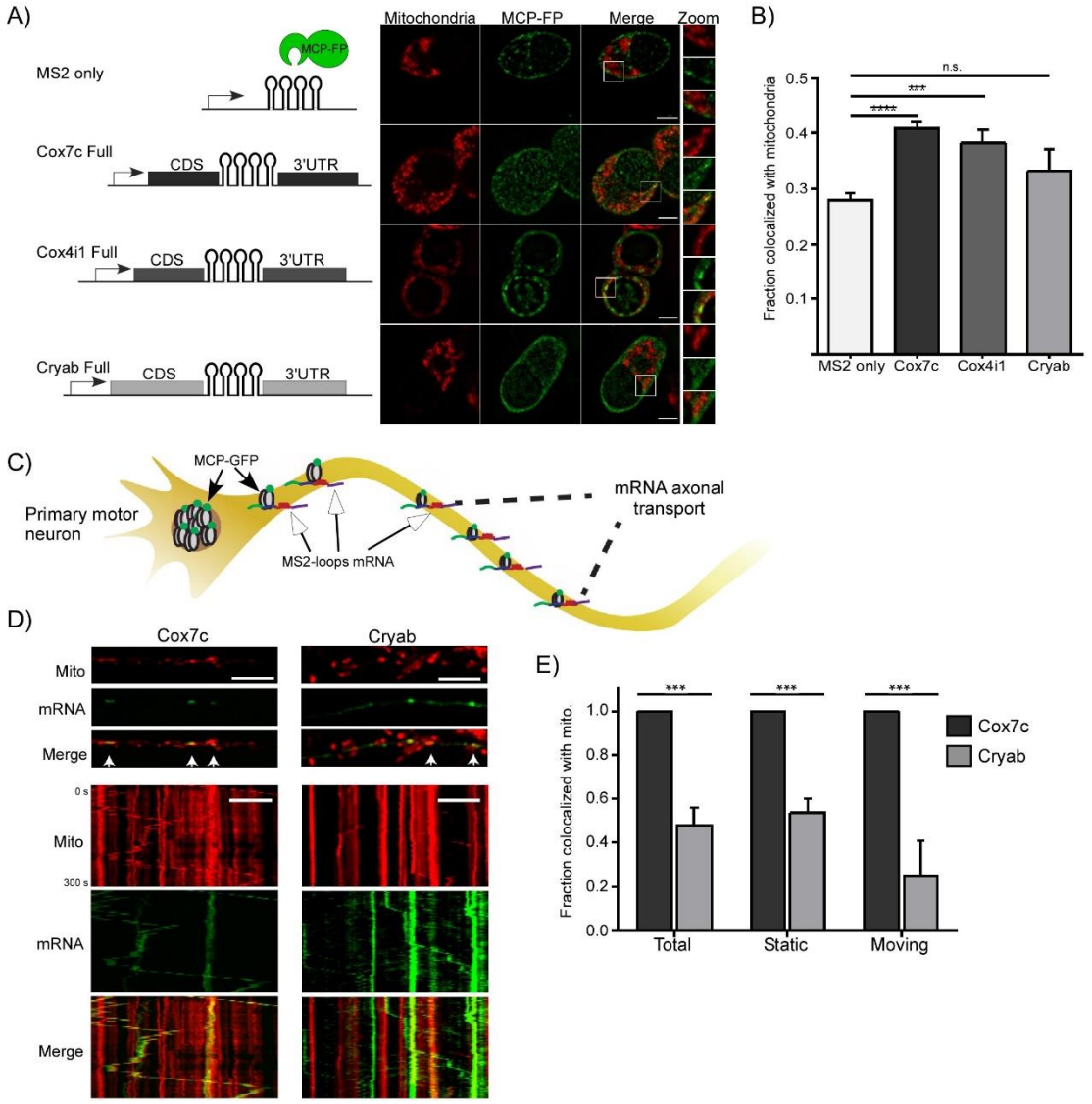

Figure 2: Live imaging reveals co-transport of mRNA with mitochondria. A) Schematic representation of the genetic constructs encoding the coding sequence (CDS) and the 3'UTR of Cox7c, Cox4i and Cryab genes, that were cloned with multiple MS2 aptamers. Representative images of the indicated MS2-mRNA constructs expressed in N2a cells together with a vector expressing MS2 binding protein fused to YFP (MCP-FP – green) co-localized with mitochondria staining (red). Scale bar = 5 µm. B) Quantification of the mRNA signal overlapping with mitochondria. Error bars are SEM. Mann-Whitney test, n.s (non-significant) $p>0.05$, ***$p<0.001$, ****$p<0.0001$, n = 34, 48, 9, 14 cells for MS2 only, Cox7c, Cox4i1 and Cryab, respectively. C) Scheme of mRNA imaging in primary motor neurons. MS2-loops containing constructs are introduced by viral infection into primary motor neurons together with a plasmid expressing GFP-tagged MS2 binding protein (MCP-GFP). Cells are grown in microfluidic chambers and signals are quantified along axonal extensions by spinning-disc microscopy. D) Representative images and kymographs of primary motor neurons infected with viral vectors expressing MCP-GFP and Cox7c or Cryab MS2-mRNA constructs (green), showing co-localization with axonal mitochondria (red). Arrowheads indicate colocalization of mRNA and mitochondria. Scale bar = 10 µm. E) Quantification of axonal co-transport between mRNA and the mitochondria separated to moving and static mRNA. Error bars are

SEM. Two-way ANOVA, ***p<0.001. n = 7 and 9 axons for Cox7c and Cryab, respectively from 3 biological independent cultures, and > 100 MS2-mRNA particles for each construct.

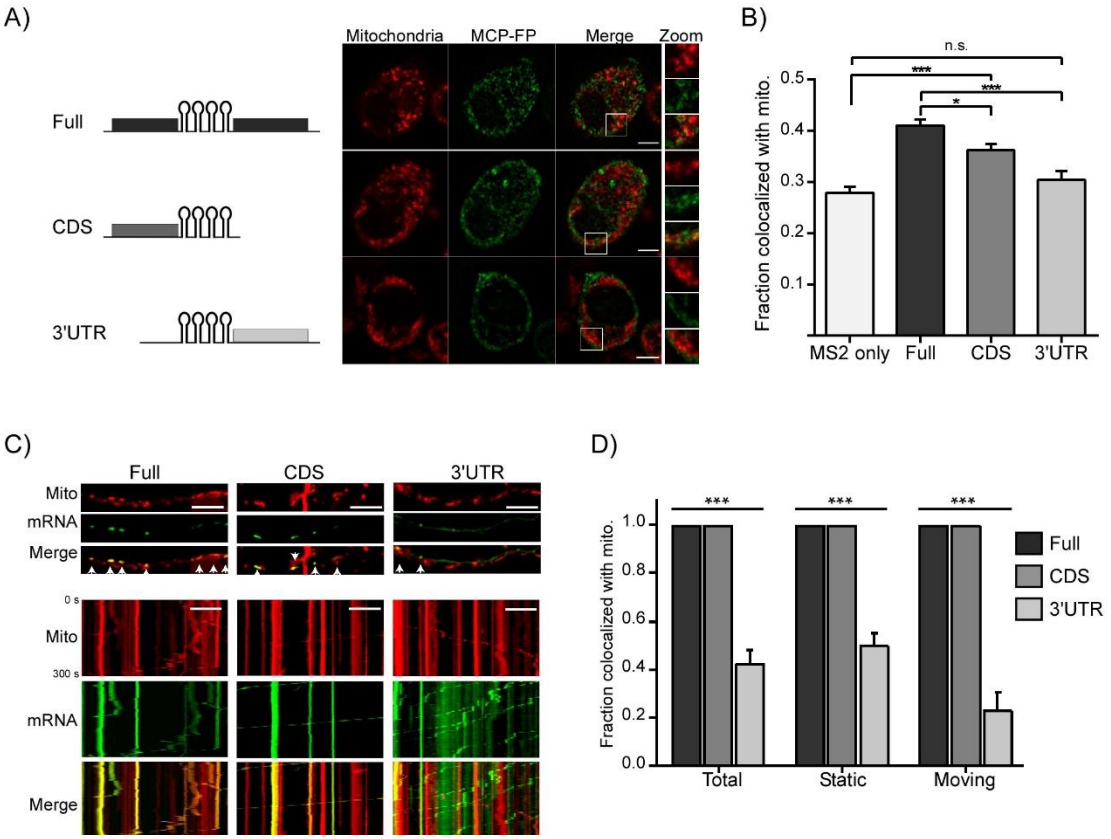

Figure 3: The coding region (CDS) contains co-localization determinants. A) Left: Schematic representation of MS2-loops constructs of the Full Cox7c, Cox7c CDS only, or Cox7c 3'UTR only. Right: Representative images of N2a cells transfected with the MS2 constructs. Scale bar = 5 µm. B) Quantification of the mRNA signal overlapping with mitochondria. Error bars are SEM. Mann-Whitney test, n.s. (non significant) p>0.05, *p<0.05, ***p<0.001, n = 23, 48, 17, 25 cells for MS2 only, Cox7c, CDS and 3'UTR, respectively. C) Images and kymographs of primary motor neurons infected with viral vectors expressing either full Cox7c, Cox7c CDS, or Cox7c 3'UTR and MCP-GFP (green). Axons show axonal colocalization with mitochondria (red) in the Full and CDS only Cox7c but not in the 3'UTR only construct. Arrowheads indicate colocalization of mitochondria and mRNA signals. Scale bar = 10 µm. D) Quantification of axonal co-transport of mRNA and mitochondria, separated to moving and static mRNA. Error bars are SEM. Two-way ANOVA, ***p<0.001. n = 8, 12, 8 axons from 3 biological independent cultures, for Cox7c full (95 particles), Cox7c CDS (215 particles) and Cox7c 3'UTR (115 particles), respectively.

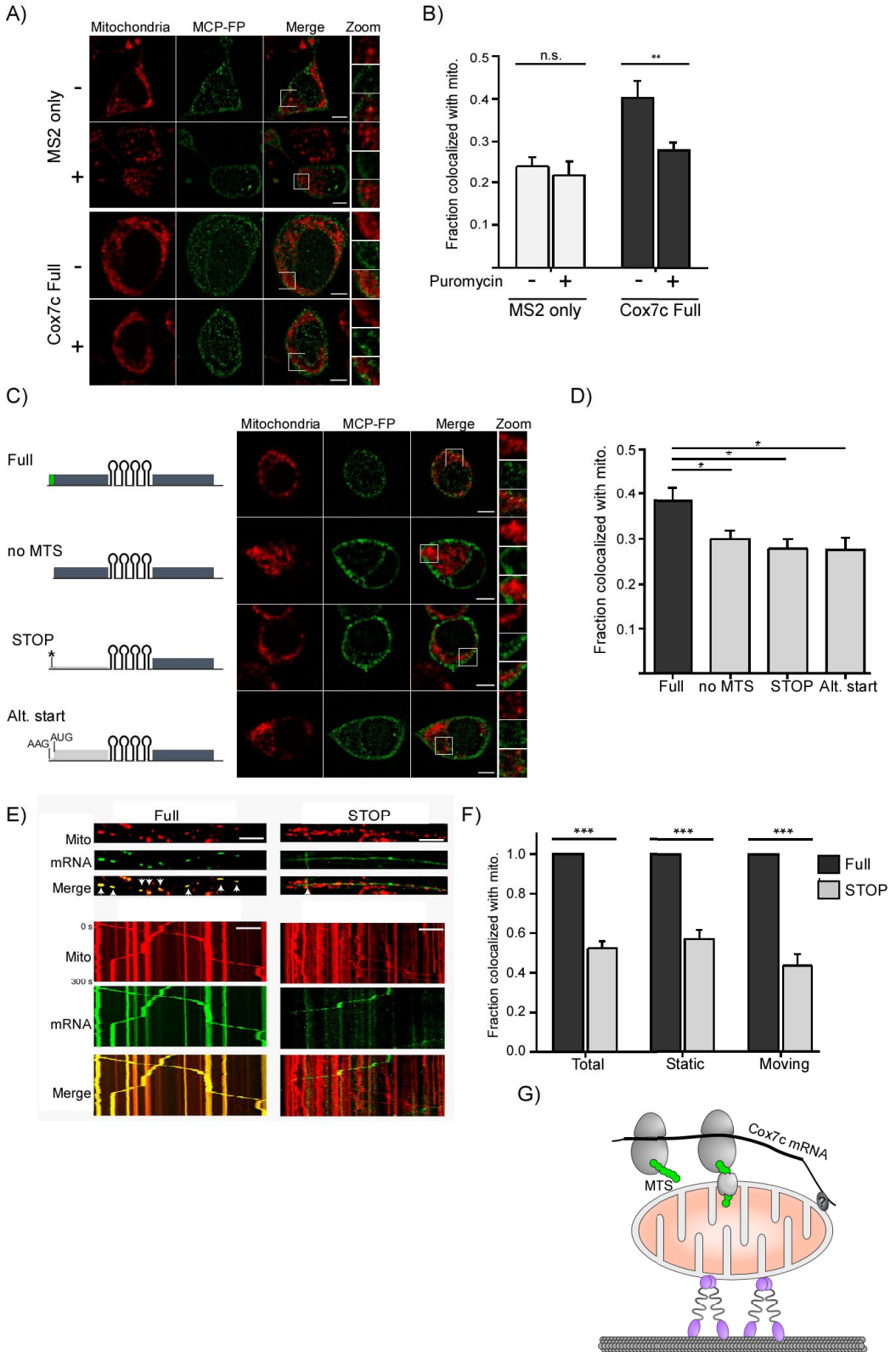

Figure 4: Translation of the MTS is important for localization. A, B) Cells transfected with the indicated plasmids were treated with the translation inhibitor puromycin (+ or -), and MCP-FP signals co-localized with mitochondria were measured. Error bars are SEM. Mann-Whitney test, n.s $p>0.05$, $**p<0.01$, n = 12, 13, 17, 19 cells for MS2-only without or with puromycin and Cox7c without or with puromycin, respectively. C) Left: Schematics of the Cox7c MTS variants used: 'no

MTS' - without 15 amino acids predicted to serve as MTS; 'STOP' – a point mutation generating a stop codon closely downstream to the initiation codon; 'Alternative Start' - point mutations that shift the start codon downstream of the MTS. Right: Representative images of co-localization with mitochondria. Scale bar = 5 μm. D) Quantification of co-localization from three independent biological repeats. Error bars are SEM. Mann-Whitney test * p <0.05. n = 14, 11, 18, 13 cells for Cox7 Full, no MTS, STOP and Alt. start, respectively. E) Images and kymographs of primary motor neurons infected with viral vectors expressing Full Cox7c or Cox7c 'STOP' and MCP-GFP (green). Axons show axonal colocalization with mitochondria (red) in the Full Cox7c but not in the Cox7c 'STOP' construct. Arrowheads indicate colocalization of mitochondria and mRNA signals. Scale bar = 10 μm. F) Quantification of axonal co-transport of mRNA and mitochondria, separated to moving and static mRNA. Error bars are SEM. Two-way ANOVA, ***p<0.001. n = 9 and 19 axons from 3 biological independent cultures, for Cox7c full (170 MS2-mRNA particles) and Cox7c 'STOP' (231 MS2-mRNA particles), respectively. G) Suggested model for co-translation-mediated mRNA transport with mitochondria. Translation of the nascent MTS (green) targets Cox7c mRNA to mitochondria and contribute to its co-transport with the organelle. Additional RNA binding proteins (denoted by '?') are likely to anchor the mRNA to the outer membrane.

References

1. W. Tan, P. Pasinelli, D. Trotti, Role of mitochondria in mutant SOD1 linked amyotrophic lateral sclerosis. *Biochim. Biophys. Acta - Mol. Basis Dis.* **1842**, 1295–1301 (2014).

2. T. Misgeld, T. L. Schwarz, Mitostasis in Neurons: Maintaining Mitochondria in an Extended Cellular Architecture. *Neuron* **96**, 651–666 (2017).

3. T. Altman, D. Geller, E. Kleeblatt, T. Gradus-Perry, E. Perlson, An in vitro compartmental system underlines the contribution of mitochondrial immobility to the ATP supply in the NMJ. *J. Cell Sci.* **132** (2019).

4. R. A. Merrill, S. Strack, Mitochondria: a kinase anchoring protein 1, a signaling platform for mitochondrial form and function. *Int. J. Biochem. Cell Biol.* **48**, 92–6 (2014).

5. Z.-H. Sheng, Mitochondrial trafficking and anchoring in neurons: New insight and implications. *J. Cell Biol.* **204**, 1087–1098 (2014).

6. M. Spillane, A. Ketschek, T. T. Merianda, J. L. Twiss, G. Gallo, Mitochondria coordinate sites of axon branching through localized intra-axonal protein synthesis. *Cell Rep.* **5**, 1564–75 (2013).

7. V. Rangaraju, M. Lauterbach, E. M. Schuman, Spatially Stable Mitochondrial Compartments Fuel Local Translation during Plasticity. *Cell* **176**, 73-84.e15 (2019).

8. N. Gershoni-Emek, *et al.*, Localization of RNAi Machinery to Axonal Branch Points and Growth Cones Is Facilitated by Mitochondria and Is Disrupted in ALS. *Front. Mol. Neurosci.* **11**, 311 (2018).

9. A. Twelvetrees, A. G. Hendricks, E. L. F. Holzbaur, SnapShot: axonal transport. *Cell* **149**, 950-950.e1 (2012).

10. M. Terenzio, G. Schiavo, M. Fainzilber, Compartmentalized Signaling in Neurons: From Cell Biology to Neuroscience. *Neuron* **96**, 667–679 (2017).

11. S. Maday, A. E. Twelvetrees, A. J. Moughamian, E. L. F. Holzbaur, Axonal Transport: Cargo-Specific Mechanisms of Motility and Regulation. *Neuron* **84**, 292–309 (2014).

12. M. Hillefors, A. E. Gioio, M. G. Mameza, B. B. Kaplan, Axon Viability and Mitochondrial Function are Dependent on Local Protein Synthesis in Sympathetic Neurons. *Cell. Mol. Neurobiol.* **27**, 701–716 (2007).

13. B. B. Kaplan, A. E. Gioio, M. Hillefors, A. Aschrafi, "Axonal Protein Synthesis and the Regulation of Local Mitochondrial Function" in *Results and Problems in Cell Differentiation*, (2009), pp. 1–25.

14. A. Aschrafi, *et al.*, MicroRNA-338 regulates local cytochrome c oxidase IV mRNA levels and oxidative phosphorylation in the axons of sympathetic neurons. *J. Neurosci.* **28**, 12581–12590 (2008).

15. A. Aschrafi, *et al.*, A heterogeneous population of nuclear-encoded mitochondrial mRNAs is present in the axons of primary sympathetic neurons. *Mitochondrion* **30**, 18–23 (2016).

16. L. F. Gumy, *et al.*, Transcriptome analysis of embryonic and adult sensory axons reveals changes in mRNA repertoire localization. *RNA* **17**, 85–98 (2011).

17. T. Shigeoka, *et al.*, Dynamic Axonal Translation in Developing and Mature Visual Circuits. *Cell* **166**, 181–192 (2016).

18. A. Minis, *et al.*, Subcellular transcriptomics-dissection of the mRNA composition in the axonal compartment of sensory neurons. *Dev. Neurobiol.* **74**, 365–81 (2014).

19. N. Rotem, *et al.*, ALS along the Axons - Expression of coding and noncoding RNA differs in axons of ALS models. *Sci. Rep.* **7** (2017).

20. Y. Kanai, N. Dohmae, N. Hirokawa, Kinesin transports RNA: Isolation and characterization of an RNA-transporting granule. *Neuron* **43**, 513–525 (2004).

21. M. Mofatteh, S. L. Bullock, SnapShot: Subcellular mRNA Localization. *Cell* **169**, 178-178.e1 (2017).

22. P. K. Sahoo, D. S. Smith, N. Perrone-Bizzozero, J. L. Twiss, Axonal mRNA transport and translation at a glance. *J. Cell Sci.* **131**, jcs196808 (2018).

23. J.-M. Cioni, *et al.*, Late Endosomes Act as mRNA Translation Platforms and Sustain Mitochondria in Axons. *Cell* **176**, 56-72.e15 (2019).

24. E. Eliyahu, C. Lesnik, Y. Arava, The protein chaperone Ssa1 affects mRNA localization to the mitochondria. *FEBS Lett.* **586**, 64–69 (2012).

25. C. Lesnik, Y. Cohen, A. Atir-Lande, M. Schuldiner, Y. Arava, OM14 is a mitochondrial receptor for cytosolic ribosomes that supports co-translational import into mitochondria. *Nat. Commun.* **5**, 5711 (2014).

26. P. Marc, *et al.*, Genome-wide analysis of mRNAs targeted to yeast mitochondria. *EMBO Rep* **3**, 159–164 (2002).

27. D. Vardi-Oknin, Y. Arava, Characterization of Factors Involved in Localized Translation Near Mitochondria by Ribosome-Proximity Labeling. *Front. cell Dev. Biol.* **7**, 305 (2019).

28. C. C. Williams, C. H. Jan, J. S. Weissman, Targeting and plasticity of mitochondrial proteins revealed by proximity-specific ribosome profiling. *Science (80-.).* **346**, 748–751 (2014).

29. A. Aschrafi, O. Natera-Naranjo, A. E. Gioio, B. B. Kaplan, Regulation of axonal trafficking of cytochrome c oxidase IV mRNA. *Mol. Cell. Neurosci.* **43**, 422–430 (2010).

30. O. Natera-Naranjo, *et al.*, Local translation of ATP synthase subunit 9 mRNA alters ATP levels and the production of ROS in the axon. *Mol. Cell. Neurosci.* **49**, 263–270 (2012).

31. B. Wu, J. A. Chao, R. H. Singer, Fluorescence fluctuation spectroscopy enables quantitative imaging of single mRNAs in living cells. *Biophys. J.* **102**, 2936–2944 (2012).

32. A. Aschrafi, *et al.*, MicroRNA-338 regulates local cytochrome c oxidase IV mRNA levels and oxidative phosphorylation in the axons of sympathetic neurons. *J. Neurosci.* **28**, 12581–12590 (2008).

33. A. N. Kar, *et al.*, Dysregulation of the axonal trafficking of nuclear-encoded mitochondrial mRNA alters neuronal mitochondrial activity and mouse behavior. *Dev. Neurobiol.* **74**, 333–350 (2014).

34. A. B. Harbauer, R. P. Zahedi, A. Sickmann, N. Pfanner, C. Meisinger, The protein import machinery of mitochondria - A regulatory hub in metabolism, stress, and disease. *Cell Metab.* **19**, 357–372 (2014).

35. E. Eliyahu, *et al.*, Tom20 mediates localization of mRNAs to mitochondria in a translation-dependent manner. *Mol. Cell. Biol.* **30**, 284–94 (2010).

36. J. J. A. Armenteros, *et al.*, Detecting sequence signals in targeting peptides using deep learning. *Life Sci. Alliance* **2** (2019).

37. N. Aviram, M. Schuldiner, Targeting and translocation of proteins to the endoplasmic reticulum at a glance. *J. Cell Sci.* **130**, 4079–4085 (2017).

38. C. Glock, M. Heumüller, E. M. Schuman, mRNA transport & local translation in neurons. *Curr. Opin. Neurobiol.* **45**, 169–177 (2017).

39. D. Schatton, E. I. Rugarli, A concert of RNA-binding proteins coordinates mitochondrial function. *Crit. Rev. Biochem. Mol. Biol.* **53**, 652–666 (2018).

40. Angelika B. Harbauer, *et al.*, Neuronal mitochondria transport Pink1 mRNA via Synaptojanin 2 to support local mitophagy. *BioXriv* (2021).

41. L. Olgeiser, *et al.*, The key protein of endosomal mRNP transport Rrm4 binds translational landmark sites of cargo mRNAs. *EMBO Rep.* **20**, e46588 (2019).

42. Y. C. Liao, *et al.*, RNA Granules Hitchhike on Lysosomes for Long-Distance

Transport, Using Annexin A11 as a Molecular Tether. *Cell* **179**, 147-164.e20 (2019).

43. A. Raj, P. van den Bogaard, S. A. Rifkin, A. van Oudenaarden, S. Tyagi, Imaging individual mRNA molecules using multiple singly labeled probes. *Nat. Methods* **5**, 877–879 (2008).

44. A. Ionescu, *et al.*, Targeting the Sigma-1 Receptor via Pridopidine Ameliorates Central Features of ALS Pathology in a SOD1G93A Model. *Cell Death Dis.* **10**, 210 (2019).